Techniques

Single-Breath-Hold Evaluation of Cardiac Function

with Use of Time-Resolved Parallel Cardiac Magnetic Resonance

Patrick Krumm, MD
Jonas D. Keuler, MD
Stefanie Mangold, MD
Tanja Zitzelsberger, MD
Christer A. Ruff, MD
Bernhard D. Klumpp, MD
Petros Martirosian, PhD
Konstantin Nikolaou, MD
Christof Burgstahler, MD
Ulrich Kramer, MD

Key words: *Breath-holding; cardiac imaging techniques/methods; heart function tests; heart ventricles/diagnostic imaging; image interpretation, computer-assisted/methods; magnetic resonance imaging, cine/methods/standards; predictive value of tests; prospective studies; reference standards; reproducibility of results; ventricular function*

From: *Section of Experimental Radiology (Dr. Martirosian), Department of Diagnostic and Interventional Radiology (Drs. Keuler, Klumpp, Kramer, Krumm, Mangold, Martirosian, Nikolaou, Ruff, and Zitzelsberger), and Department of Internal Medicine V, Sports Medicine (Dr. Burgstahler), University of Tübingen, 72076 Tübingen, Germany*

Dr. Keuler is now at the Department of Anesthesiology, Marienhospital Stuttgart, Stuttgart, Germany.

Address for reprints: *Patrick Krumm, MD, Department of Diagnostic and Interventional Radiology, University of Tübingen, Hoppe-Seyler-Str. 3, 72076 Tübingen, Germany*

E-mail: *patrick.krumm@uni-tuebingen.de*

Using cardiac magnetic resonance, we tested whether a single-breath-hold approach to cardiac functional evaluation was equivalent to the established multiple-breath-hold method.

We examined 39 healthy volunteers (mean age, 31.9 ± 11.4 yr; 22 men) by using 1.5 T with multiple breath-holds and our proposed single breath-hold. Left ventricular and right ventricular ejection fractions (LVEF and RVEF), LV and RV end-diastolic volumes (LVEDV and RVEDV), and LV myocardial mass (LVMM) were compared by using Bland-Altman plots; LVEF and RVEF were tested for equivalence by inclusion of 95% confidence intervals (CIs). Equivalence of the methods was assumed within the range of –5% to 5%.

In the multiple- versus the single-breath-hold method, LVEF was 0.62 ± 0.05 versus 0.62 ± 0.04, and RVEF was 0.59 ± 0.06 versus 0.59 ± 0.07. The mean difference in both methods was –0.2% (95% CI, –1 to 0.6) for LVEF and 0.3% (95% CI, –0.8 to 1.5) for RVEF. The mean differences between methods fit within the predetermined range of equivalence, including the 95% CI. The mean relative differences between the methods were 3.8% for LVEDV, 4.5% for RVEDV, and 1.6% for LVMM.

Results of our single-breath-hold method to evaluate LVEF and RVEF were equivalent to those of the multiple-breath-hold technique. In addition, LVEDV, RVEDV, and LVMM showed low bias between methods. ***(Tex Heart Inst J 2017;44(4):252-9)***

Quantifying cardiac function is crucial for diagnosis and therapeutic decisions in many cardiac diseases. Functional measurements such as ejection fraction, end-diastolic volume, end-systolic volume, and stroke volume, along with myocardial mass, are independent predictors of cardiac morbidity and death.[1-3] In cases of arrhythmogenic right ventricular cardiomyopathy (ARVC)[4] and congenital heart diseases, right ventricular (RV) functional criteria are essential to definitively diagnose the condition and to predict outcome.[5]

Cardiac magnetic resonance (CMR) is highly useful for evaluating cardiac function[6] because of its high temporal and spatial resolution and its independence from superposition and viewing windows.[7] In addition, cardiac structures such as the ventricular apices are difficult to depict echocardiographically. Cardiac magnetic resonance, which is relatively unaffected by body habitus and limited only by the diameter of the bore and flat bedding, yields low intra- and interobserver variability.[8]

The best CMR approach for determining cardiac function combines disk-shaped volumes in short-axis view and steady-state free-precession (SSFP) cine images acquired during several breath-holds (BHs).[9] The summation of disks, called the modified Simpson method, is independent from geometric assumptions[10]; this is particularly important in patients with diseased myocardium because of postischemic, pathologically altered ventricular geometry and pathologic asymmetric contractility.[11] To obtain optimal volumetric measurements in a stack of short-axis slices, the slice thickness and gaps between slices should be minimal, and the temporal resolution of the cine imaging should be kept in optimal range—all with a reasonable balance of BH time and slices obtained per BH. In established sequence protocols, 8 to 12 BHs of 10 to 15 s each are necessary to examine the entire left ventricle (LV).[7] Assuming 10 s of recov-

This study was supported by a grant from the German Heart Foundation (F/10/09).

ery time for the patient between each BH, this method of quantifying cardiac function can take as long as 5 min.[12] A patient's inability to follow BH instructions can necessitate repeating the study.

The temporal generalized autocalibrating partially parallel acquisitions (T-GRAPPA) acceleration technique has been applied to real-time dynamic cardiac imaging.[13] In T-GRAPPA, a time-interleaved acquisition scheme is used to obtain coil sensitivity maps directly from the actual dynamic acquisition data.[14] This eliminates the need to obtain additional reference data separately and enables full image acceleration.

The aim of our study was to compare cardiac functional results from T-GRAPPA–accelerated SSFP cine imaging during a single BH with those of SSFP cine images acquired during multiple BHs. The main variables were LV ejection fraction (LVEF) and RV ejection fraction (RVEF).

Study Population and Methods

We prospectively examined 39 healthy, athletic volunteers (mean age, 31.9 ± 11.4 yr; 22 men) (Table I). The study protocol was advised and approved by the local review ethics board, and all participants gave written informed consent.

Image Acquisition

We performed CMR by using a 1.5-Tesla MAGNETOM® Avanto magnetic resonance scanner (Siemens Healthcare GmbH; Erlangen, Germany), equipped with a gradient system that had a maximal strength of 45 mT/m and a maximal slew rate of 200 T/m/s. A 6-channel body-array coil and 6 elements of a spine coil were used for signal reception.

The BH sequences consisted of prospectively triggered, 2-dimensional SSFP cine images. The reference (multiple-BH) sequence acquired 2 short-axis slices per BH. The scanner calculated a fixed 22 phases of the cardiac cycle. In contrast, the study sequence acquired all short-axis slices necessary to determine ventricular volume, from base to apex, during a single BH. In this protocol, calculated phases of the cardiac cycle depended on the number of segments that could be read per R-R interval and on individual heart rate, required number of slices, and a 20-s limit for BH duration. Each study participant was examined serially during a single CMR session and underwent multiple- and single-BH acquisition in a random order, to avoid influence by the order of examination. Table II shows details of the sequences.

TABLE I. Demographic Characteristics of the Study Population

Variable	Value
Age (yr)	31.9 ± 11.4 (19–62)
Height (cm)	176.2 ± 9 (160–198)
Weight (kg)	68.7 ± 11.7 (51–97)
Body surface area (m^2)	1.83 ± 0.19 (1.51–2.27)
Body mass index (kg/m^2)	22.1 ± 2.6 (18.3–30)
Heart rate (beats/min)	66 ± 18 (47–113)

Data are presented as mean ± SD and range.

Image Analysis

Image analysis was performed on a *syngo*® Multimodality Workplace (Siemens Healthcare) by 2 independent, blinded observers (JDK and PK; 1 and 4 yr of experience in cardiac imaging, respectively). They were blinded to their own results, by evaluating one method in an individual and then evaluating the second method on a different day. To evaluate ventricular volumes, the endocardial contours were manually drawn in end-diastolic and end-systolic phases. To evaluate LV myocardial mass (LVMM), the LV epicardial contours were drawn manually; the septum was included in LVMM by convention, and RV trabecula arising from the septum were excluded. The papillary muscles were not excluded from the cavum. The basal slice was integrated into the LV cavum if the LV myocardium exceeded 180° of the myocardial circumference. Apical slices with no

TABLE II. Sequence Settings in the Multiple- and Single-Breath-Hold Methods

Variable	Multiple-Breath-Hold	Single-Breath-Hold
Repetition time (ms)	60.6	55.4
Echo time (ms)	1.2	1.1
Flip angle	80°	75°
Matrix (phase encodings × frequency encodings)	113 × 192	101 × 192
Pixel size (mm^2)	1 × 0.7 – 2.2 × 1.7	1.1 × 0.7 – 2.5 × 1.8
Temporal resolution (ms)	45	55
Receiver bandwidth (Hz/pixel)	930	789
Slice thickness (mm)	5	6
Gap (mm)	5	6
Parallel imaging acceleration factor	GRAPPA 2	T-GRAPPA 2

(T-)GRAPPA = (temporal) generalized autocalibrating partially parallel acquisitions

detectable cavity were excluded from evaluation. Right ventricular trabeculations were included in the cavity volume. The following morphologic and functional characteristics of the LV were calculated with Argus postprocessing software (Siemens Healthcare): end-diastolic volume (LVEDV), end-systolic volume (LVESV), stroke volume (LVSV), ejection fraction (LVEF), and LVMM, as well as the body surface–normalized index values for those variables. Except for RV myocardial mass, the corresponding RV characteristics and indices were also evaluated. The number of slices taken into account, number of phases per cardiac cycle, and total acquisition times for both methods were recorded.

Image quality was rated quantitatively: the coefficient of variation (CV) of the CMR signal was measured in a standardized 15-mm^2 region of interest in the inferoseptal myocardium and the LV blood pool, respectively. The CV was calculated from absolute CMR signal S and its SD σ as follows:

$$CV = \frac{\sigma}{S},$$

with 0 as the minimum possible CV value and 1 as the theoretical maximum. The CMR contrast signal between the inferoseptal myocardium and LV blood pool was calculated as follows:

$$Contrast = \frac{S_{blood\ pool} - S_{myocardium}}{S_{blood\ pool} + S_{myocardium}},$$

with 1 indicating maximum possible contrast and 0 indicating no contrast.

Statistical Analysis

Statistical analysis was performed by using JMP® version 11.2 (SAS Institute Inc.; Cary, NC). Bland-Altman plots with ±1.96 SD limits of agreement were created with use of Prism® version 7.03 (GraphPad Software, Inc.; La Jolla, Calif). Continuous variables are expressed as mean ± SD with additional range.

The most clinically relevant quantitative cardiac functional values, LVEF and RVEF, were the primary targets compared between the 2 methods and tested for equivalence. To prove equivalence, the "inclusion of 95% confidence intervals" (CIs) method was performed.[15]

Initially, we had defined a range of equivalence of ±5%, to determine which difference should not be relevant and acceptable in clinical routine. By this definition, equivalence of the 2 methods was assumed if the difference of the results of both methods was within the range of –5% to 5%.

Bland-Altman plots of LVEF, RVEF, LVEDV, RV end-diastolic volume (RVEDV), and LVMM were created in percentages, to facilitate determining agreement between the methods. Differences were calculated as $LVEF_{single\ BH} - LVEF_{multiple\ BH}$, and averages as $(LVEF_{single\ BH} - LVEF_{multiple\ BH})/2$. The 2-sided $100(1–2\alpha)\%$ CI for the difference between the LVEF values of the multiple- and single-BH sequences ($LVEF_{single\ BH} - LVEF_{multiple\ BH}$) was calculated, and the level of significance was set to α=5%. Equivalence of the 2 methods was assumed if the 95% CI for the difference $LVEF_{single\ BH} - LVEF_{multiple\ BH}$ fit within the predetermined range of equivalence (–5% to 5%). The RVEF was evaluated in the same fashion. The mean intraindividual interventricular difference of LVSV and RVSV was evaluated by using Bland-Altman plots for each method; this excluded different absolute stroke volumes within one individual and method. Interobserver variability was evaluated for LVEF and RVEF by using Bland-Altman plots for both methods. To avoid multiple testing, we performed no further statistical tests for equivalence or difference of other values. A descriptive statistic was applied for all other functional values.

Results

Endocardial contours were evaluable in all data sets. Figure 1 shows representative short-axis slices acquired via both methods. Table III shows detailed volumetric data, acquisition times for each method, and quantitative image quality. The LVEF was 0.62 ± 0.05 for the multiple-BH sequence and 0.62 ± 0.04 for the single-BH sequence. The RVEF was 0.59 ± 0.06 for the multiple sequence and 0.59 ± 0.07 for the single-BH sequence. The intraindividual mean interventricular difference between LVSV and RVSV was 1 ± 5.4 mL for the multiple-BH sequence and 0.3 ± 10.2 mL for the single-BH sequence.

Comparison of the Methods

The Bland-Altman plots showed mean differences between both methods of –0.2% (limits of agreement, –5.2% to 4.7%) for LVEF (Fig. 2A) and 0.3% (limits of agreement, –6.4% to 7.1%) for RVEF (Fig. 2B). The lower and higher 95% CIs of –1 and 0.6 for LVEF, and those of –0.8 and 1.5 for RVEF, fit within the predetermined range of equivalence.

The mean relative difference between both methods for LVEDV was 3.8% (limits of agreement, –4.7% to 12%). For RVEDV, this was 4.5% (limits of agreement, –15% to 24%). For LVMM, the difference was 1.6% (limits of agreement, –9.7% to 13%).

Interobserver Variability

For LVEF, interobserver bias in the multiple-BH method was 0.13% (limits of agreement, –3.9% to 4.2%), and bias in the single-BH method was –0.12% (limits of agreement, –4.3% to 4.1%). For RVEF, interobserver bias in the multiple-BH method was 0.71% (limits of agreement, –8.5% to 9.9%), and bias in the single-BH method was 1.1% (limits of agreement, –7.5% to 9.8%).

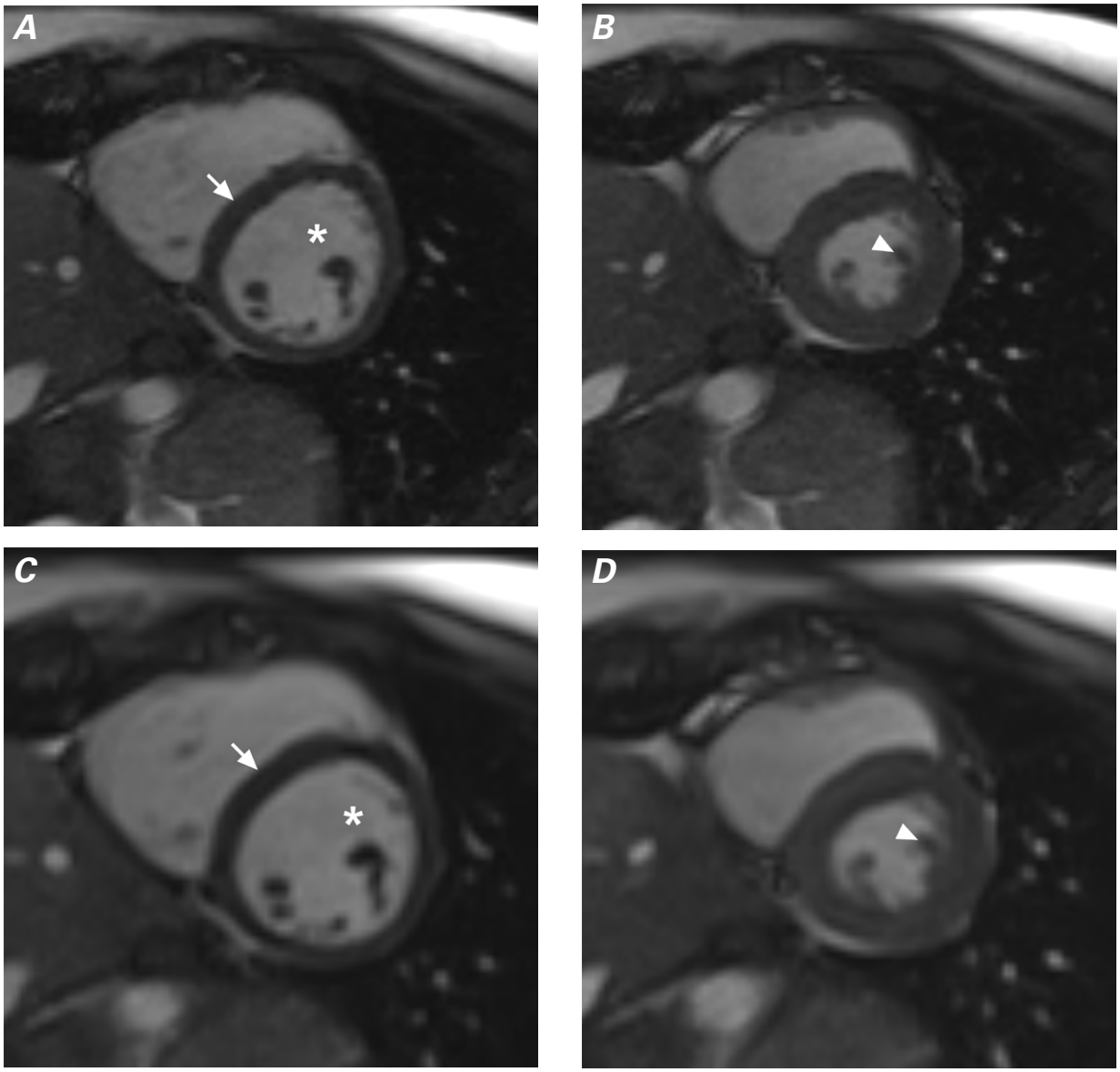

Fig. 1 *Cardiac magnetic resonance images with steady-state free precession show representative midventricular short-axis slices acquired in* ***A****,* ***B****) multiple- and* ***C****,* ***D****) single-breath-hold sequences during* ***A****,* ***C****) end-diastole and* ***B****,* ***D****) end-systole. Signals were measured for the inferoseptal myocardium (arrows) and left ventricular blood pool (asterisks). Left ventricular trabeculae (arrowheads) were depicted similarly in both methods without visually apparent differences in image quality.*

Discussion

Economical use of time in CMR evaluation of cardiac function is important in clinical practice. Whereas enough time should be allocated for morphologic and viability evaluations, scanning time should be minimized for patients' comfort. Left ventricular ejection fraction is an important criterion for decision-making in therapy and as a predictor of outcome.[16,17] In the current study, a T-GRAPPA–accelerated approach for evaluating LV cardiac function during a single BH was compared with the established multiple-BH protocol. We tested the equivalence of the 2 methods, versus merely testing statistical differences and assuming equivalence. Our results indicate that the single-BH method is as effective as the multiple-BH method for evaluating cardiac function: in tests for equivalence, the mean difference for LVEF and RVEF in both methods was close to 0, and the 95% CI fit within the predetermined range of equivalence. In terms of clinical relevance, our method of evaluating LVEF and RVEF yields results as accurate as those of the reference standard.[18] For the other LV variables, we observed good agreement between both methods without statistical testing. The absolute cardiac volumes were slightly underestimated in the single-BH method, which can be attributed to reduced accuracy in the most basal and apical slices. This prob-

TABLE III. Comparison of Volumetric and Imaging Results in the Multiple- and Single-Breath-Hold Methods

Variable	Multiple-Breath-Hold	Single-Breath-Hold
LVEDV (mL)	167.7 ± 44	161.6 ± 42.6
LVESV (mL)	64 ± 20.1	62.1 ± 20
LVSV (mL)	103.7 ± 25.6	99.5 ± 24.6
LVEF	0.62 ± 0.05	0.62 ± 0.04
LVMM (g)	132.2 ± 42.4	129.9 ± 41.4
LVEDV index (mL/m^2)	90.2 ± 16.8	86.8 ± 16.3
LVESV index (mL/m^2)	34.3 ± 8.5	33.3 ± 8.2
LVSV index (mL/m^2)	55.8 ± 10.2	53.6 ± 9.6
LVMM index (g/m^2)	70.9 ± 18.6	69.7 ± 17.8
RVEDV (mL)	176.9 ± 57.8	168.2 ± 51.5
RVESV (mL)	75.1 ± 32	70.5 ± 27.4
RVSV (mL)	101.8 ± 28.4	97.6 ± 27.3
RVEF	0.59 ± 0.06	0.59 ± 0.07
RVEDV index (mL/m^2)	94.8 ± 24.5	90.2 ± 22.1
RVESV index (mL/m^2)	40 ± 14.5	37.7 ± 12.6
RVSV index (mL/m^2)	54.7 ± 11.7	52.6 ± 11.7
Intraindividual mean interventricular difference (mL)	1 ± 5.4	0.3 ± 10.2
LV slices in end-diastole (n)	9.5 ± 0.9 (8–11)	7.6 ± 0.6 (6–8)
Phases per cardiac cycle (n)	22	17.3 ± 3.9 (11–26)
Total acquisition time (s)	190.3 ± 64	22.4 ± 9
CV in inferoseptal myocardium	0.08 ± 0.04	0.1 ± 0.08
CV in LV blood pool	0.02 ± 0.01	0.02 ± 0.01
Contrast between inferoseptalmyocardium and LV blood pool	0.6 ± 0.1	0.6 ± 0.1

CV = coefficient of signal variation; LV = left ventricular; LVEDV = left ventricular end-diastolic volume; LVEF = left ventricular ejection fraction; LVESV = left ventricular end-systolic volume; LVMM = left ventricular myocardial mass; LVSV = left ventricular stroke volume; RVEDV = right ventricular end-diastolic volume; RVEF = right ventricular ejection fraction; RVESV = right ventricular end-systolic volume; RVSV = right ventricular stroke volume

Data are expressed as mean ± SD for continuous variables and as mean ± SD and range for discrete variables.

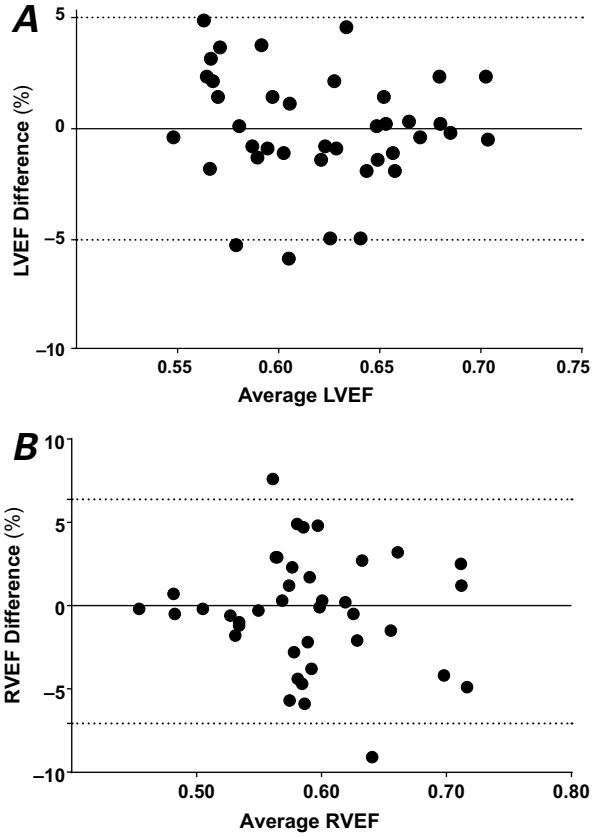

Fig. 2 *Bland-Altman plots show good agreement of **A**) left ventricular ejection fraction (LVEF) and **B**) right ventricular ejection fraction (RVEF) as determined by means of the standard multiple-breath-hold and the temporal generalized autocalibrating partially parallel acquisition (T-GRAPPA) single-breath-hold methods. The mean difference is represented by the continuous bold lines close to 0, indicating good agreement of both methods. The dotted lines represent the limits of agreement at ± 1.96 SD. The dots indicate intraindividual measurement for both methods. The closer to 0 all dots and the bold mean-difference line, the better the agreement of the methods. Systematic over- or underestimation would be indicated by a mean-difference line far from 0.*

lem is known to markedly influence LV volumetric values.[19] Our results are concordant with those of other reported single-BH techniques.[20,21] Previous investigators had different statistical approaches: they tested for statistically significant differences and assumed equality if none was found. If a study was underpowered, the level of significant difference might not be achieved only for lack of sample size.

Planning of slice acquisition should be done carefully, to ensure that basal slices in end-diastole are included. In any compromise regarding the possible number of slices, the most basal slice should never be excluded, because the longitudinal ventricular contraction contributes largely to the ejection fraction.[22] In contrast, the apex shows only minimal longitudinal contraction, and the minor volume ejected by the apical cone can be omitted without relevant bias to the LVSV and LVEF.

The low intraindividual mean interventricular difference of the LVSVs and RVSVs (approximately 1 mL) that occurred in both sequences still enabled consistent

evaluation. Higher variation for RV functional values within individuals was to be expected in the single-BH approach, which was designed for and dedicated to LV evaluation. The bias for RV end-diastolic values might be relevant for exact RV evaluations in ARVC and in congenital heart disease.[23-25] Cardiac magnetic resonance is the reference method for RV evaluation, but it is dependent on the acquisition of basal RV slices, which can easily be missed if the focus is only on the mitral valve plane, as is the case with most basal slices.[26] The tricuspid valve and pulmonary valve planes are below the mitral valve plane, and those 2 planes are rotated. The large area of the basal slices in the RV—including the RV outflow tract—makes it difficult to determine the most basal slice of the RV.[27]

For LV evaluation, we set the short-axis orientation parallel to the mitral valve and perpendicular to the ventricular septum. Even though this LV short axis does not represent the true RV short axis, RV evaluation is generally possible in the dedicated LV short-axis view. In contrast, Alfakih and colleagues[28] have recommended the quantification of RV function from strictly axial slices. Because of a need for reproducible follow-up functional evaluation of the RV, this short-axis, single-BH approach is not recommended for RV evaluation in ARVC or congenital heart disease.[25]

Our interobserver variability—good in both methods—was slightly higher in the single-BH approach. Fewer but thicker slices with a greater gap obviously complicate determining the basal slice, potentially reducing the reproducibility of volumetry.[19]

Signal and contrast were quantified relatively, because signal-to-noise ratio measurements in *k*-space–undersampling accelerated methods are not possible by means of a measurement in the tissue of interest and in the image background.[29,30] In myocardial and blood-pool contrast, the CV was close to the ideal value of 0 for both methods. The image contrast was similar for both methods and was acceptable at 0.6 ± 0.01. Experimental and quantitative approaches have revealed that T-GRAPPA has only minor effects on temporal resolution and noise behavior and can even compensate for breathing artifacts.[13] In addition, T-GRAPPA has yielded acceptable results in new free-breathing techniques.[31] Hence, T-GRAPPA–accelerated SSFP cine imaging sequences might also reduce recording time for other approaches that involve single-slice or multislice cardiac sequences, with little or no visible reduction in image quality.

Our proposed single-BH method shortens examination time. The entire short-axis stack is acquired within 20 s, in comparison with repetitive BHs of 10 to 15 s each, plus resting time, for up to 5 min total. Some authors have characterized CMR as a non-real-time method that acquires functional values within minutes rather than seconds,[10] leading to artifacts caused by changing cardiac physiology and different depths of breath, during which the disk shapes can shift. Inaccuracies caused by shifting slices are certainly higher in axial than in short-axis volumetry. An optimized axial single-BH method might avoid errors in RV functional evaluation caused by different depths of breath. The single-BH protocol acquires all data in 15 to 30 consecutive cardiac cycles, enabling cardiac function to be evaluated under consistent physiologic conditions. Lower temporal resolution in the single-BH method, however, can make evaluating wall motion more difficult. In patients whose BH ability is poor, our method enables stitching 2 or more BH concatenations, which still allows for shorter BH times with higher temporal and spatial resolution. This capability might prove more useful than fitting acquisition into one BH, especially during acquisition of axial views in pediatric cardiology for RV evaluation. If no BH is possible, T-GRAPPA–accelerated free-breathing real-time images are an option.[31]

Limitations of the Study

A limitation of this study is that only healthy volunteers who were capable of long BHs were examined. Severely ill patients probably cannot hold their breath for 20 to 30 s for the single-BH whole-ventricle sequence. Because of adaption to athleticism, many of our study participants had larger LVs than those in typical sedentary patients.[32,33] However, in comparison with our study population, many patients have much larger hearts that are distorted for a variety of reasons, including prior myocardial infarction, valvular heart disease, pulmonary hypertension, and congenital heart disease. In heart failure, CMR is generally limited in comparison with echocardiography, because of flat bedding. Finally, the prospective triggering of both methods in this study might cut out end-diastolic phases; however, this effect is reportedly only of minor influence.[34]

Conclusion

As a temporal *k*-space–based parallel imaging method, T-GRAPPA enables the acquisition of all LV short-axis slices for cardiac functional evaluation during a single BH, and it shortens examination time. We conclude that the results of single-BH, T-GRAPPA–accelerated, whole-ventricle evaluation of LVEF and RVEF are equivalent to those of the established multiple-BH acquisition method.

References

1. Kindermann I, Kindermann M, Kandolf R, Klingel K, Bultmann B, Muller T, et al. Predictors of outcome in patients with suspected myocarditis [published erratum appears in Circulation 2008;118(12):e493]. Circulation 2008;118(6):639-48.
2. Reinstadler SJ, Klug G, Feistritzer HJ, Kofler M, Pernter B, Gobel G, et al. Prognostic value of left ventricular global func-

tion index in patients after ST-segment elevation myocardial infarction. Eur Heart J Cardiovasc Imaging 2016;17(2):169-76.
3. van der Vleuten PA, Rasoul S, Huurnink W, van der Horst IC, Slart RH, Reiffers S, et al. The importance of left ventricular function for long-term outcome after primary percutaneous coronary intervention. BMC Cardiovasc Disord 2008; 8:4.
4. Marcus FI, McKenna WJ, Sherrill D, Basso C, Bauce B, Bluemke DA, et al. Diagnosis of arrhythmogenic right ventricular cardiomyopathy/dysplasia: proposed modification of the Task Force Criteria. Eur Heart J 2010;31(7):806-14.
5. Kotani Y, Chetan D, Ono N, Mertens LL, Caldarone CA, Van Arsdell GS, Honjo O. Late functional outcomes after repair of tetralogy of Fallot with atrioventricular septal defect: a double case-match control study. J Thorac Cardiovasc Surg 2013;145(6):1477-84, 1484.e1-4.
6. Wintersperger BJ, Bamberg F, De Cecco CN. Cardiovascular imaging: the past and the future, perspectives in computed tomography and magnetic resonance imaging. Invest Radiol 2015;50(9):557-70.
7. Hazirolan T, Tasbas B, Dagoglu MG, Canyigit M, Abali G, Aytemir K, et al. Comparison of short and long axis methods in cardiac MR imaging and echocardiography for left ventricular function. Diagn Interv Radiol 2007;13(1):33-8.
8. Danilouchkine MG, Westenberg JJ, de Roos A, Reiber JH, Lelieveldt BP. Operator induced variability in cardiovascular MR: left ventricular measurements and their reproducibility. J Cardiovasc Magn Reson 2005;7(2):447-57.
9. Grebe O, Kestler HA, Merkle N, Wohrle J, Kochs M, Hoher M, Hombach V. Assessment of left ventricular function with steady-state-free-precession magnetic resonance imaging. Reference values and a comparison to left ventriculography. Z Kardiol 2004;93(9):686-95.
10. Dulce MC, Mostbeck GH, Friese KK, Caputo GR, Higgins CB. Quantification of the left ventricular volumes and function with cine MR imaging: comparison of geometric models with three-dimensional data. Radiology 1993;188(2):371-6.
11. Bellenger NG, Burgess MI, Ray SG, Lahiri A, Coats AJ, Cleland JG, Pennell DJ. Comparison of left ventricular ejection fraction and volumes in heart failure by echocardiography, radionuclide ventriculography and cardiovascular magnetic resonance; are they interchangeable? Eur Heart J 2000;21(16): 1387-96.
12. Theisen D, Sandner TA, Bamberg F, Bauner KU, Schwab F, Schwarz F, et al. High-resolution cine MRI with TGRAPPA for fast assessment of left ventricular function at 3 Tesla. Eur J Radiol 2013;82(5):e219-24.
13. Breuer FA, Kellman P, Griswold MA, Jakob PM. Dynamic autocalibrated parallel imaging using temporal GRAPPA (TGRAPPA). Magn Reson Med 2005;53(4):981-5.
14. Griswold MA, Jakob PM, Heidemann RM, Nittka M, Jellus V, Wang J, et al. Generalized autocalibrating partially parallel acquisitions (GRAPPA). Magn Reson Med 2002;47(6):1202-10.
15. Westlake WJ. Use of confidence intervals in analysis of comparative bioavailability trials. J Pharm Sci 1972;61(8):1340-1.
16. Catalano O, Moro G, Perotti M, Frascaroli M, Ceresa M, Antonaci S, et al. Late gadolinium enhancement by cardiovascular magnetic resonance is complementary to left ventricle ejection fraction in predicting prognosis of patients with stable coronary artery disease. J Cardiovasc Magn Reson 2012; 14:29.
17. Grun S, Schumm J, Greulich S, Wagner A, Schneider S, Bruder O, et al. Long-term follow-up of biopsy-proven viral myocarditis: predictors of mortality and incomplete recovery. J Am Coll Cardiol 2012;59(18):1604-15.
18. Higgins CB. Which standard has the gold? J Am Coll Cardiol 1992;19(7):1608-9.
19. Groth M, Muellerleile K, Klink T, Saring D, Halaj S, Folwarski G, et al. Improved agreement between experienced and inexperienced observers using a standardized evaluation protocol for cardiac volumetry and infarct size measurement. Rofo 2012;184(12):1131-7.
20. Nassenstein K, Eberle H, Maderwald S, Jensen CJ, Heilmaier C, Schlosser T, Bruder O. Single breath-hold magnetic resonance cine imaging for fast assessment of global and regional left ventricular function in clinical routine. Eur Radiol 2010; 20(10):2341-7.
21. Eberle HC, Nassenstein K, Jensen CJ, Schlosser T, Sabin GV, Naber CK, Bruder O. Rapid MR assessment of left ventricular systolic function after acute myocardial infarction using single breath-hold cine imaging with the temporal parallel acquisition technique (TPAT) and 4D guide-point modelling analysis of left ventricular function. Eur Radiol 2010;20 (1):73-80.
22. Maciver DH. The relative impact of circumferential and longitudinal shortening on left ventricular ejection fraction and stroke volume. Exp Clin Cardiol 2012;17(1):5-11.
23. Hunold P. MRI for arrhythmogenic right ventricular dysplasia/cardiomyopathy (ARVD/C) [in German]. Radiologe 2013;53(1):38-44.
24. Achenbach S, Barkhausen J, Beer M, Beerbaum P, Dill T, Eichhorn J, et al. Consensus recommendations of the German Radiology Society (DRG), the German Cardiac Society (DGK) and the German Society for Pediatric Cardiology (DGPK) on the use of cardiac imaging with computed tomography and magnetic resonance imaging [in German]. Rofo 2012;184(4):345-68.
25. Weiss F, Habermann CR, Lilje C, Weil J, Adam G. MRI of congenital heart disease in childhood [in German]. Rofo 2004;176(2):191-9.
26. Johnson TR, Hoch M, Huber A, Romer U, Reiser MF, Schonberg SO, Netz H. Quantification of right ventricular function in congenital heart disease: correlation of 3D echocardiography and MRI as complementary methods [in German]. Rofo 2006;178(10):1014-21.
27. Grothues F, Moon JC, Bellenger NG, Smith GS, Klein HU, Pennell DJ. Interstudy reproducibility of right ventricular volumes, function, and mass with cardiovascular magnetic resonance. Am Heart J 2004;147(2):218-23.
28. Alfakih K, Plein S, Bloomer T, Jones T, Ridgway J, Sivananthan M. Comparison of right ventricular volume measurements between axial and short axis orientation using steady-state free precession magnetic resonance imaging. J Magn Reson Imaging 2003;18(1):25-32.
29. Dietrich O, Raya JG, Reeder SB, Reiser MF, Schoenberg SO. Measurement of signal-to-noise ratios in MR images: influence of multichannel coils, parallel imaging, and reconstruction filters. J Magn Reson Imaging 2007;26(2):375-85.
30. Binter C, Ramb R, Jung B, Kozerke S. A g-factor metric for k-t SENSE and k-t PCA based parallel imaging. Magn Reson Med 2016;75(2):562-71.
31. Schwab F, Schwarz F, Dietrich O, Lanz T, Resmer F, Wichmann T, et al. Free breathing real-time cardiac cine imaging with improved spatial resolution at 3 T. Invest Radiol 2013;48 (3):158-66.
32. Kramer U, Mangold S, Krumm P, Seeger A, Franzen E, Niess AM, et al. Determination of morphological and functional adaptations in top level female handball players using cardiac MR imaging [in German]. Dtsch Z Sportmed 2013;64(11): 333-8. Available from: http://www.zeitschrift-sportmedizin.de/fileadmin/content/archiv2013/Heft_11/originalia_kramer.pdf.

33. Mangold S, Kramer U, Franzen E, Erz G, Bretschneider C, Seeger A, et al. Detection of cardiovascular disease in elite athletes using cardiac magnetic resonance imaging. Rofo 2013;185(12):1167-74.
34. Heijman E, de Graaf W, Niessen P, Nauerth A, van Eys G, de Graaf L, et al. Comparison between prospective and retrospective triggering for mouse cardiac MRI. NMR Biomed 2007;20(4):439-47.